



OPEN Research of the clinical features, risk factors, and surgical diagnosis of intramural stones in patients with gallbladder stones

Xiaobing Luo¹✉, Hongying Cai², Xiaofeng Wang³, Ruihong Ma¹, Gang Wang³, Sangui Wang⁴✉ & Tie Qiao⁵✉

Crystals or stones within the gallbladder wall in patients with gallbladder stones (GBS) have been occasionally reported, but their clinical features and aetiology remain unclear. This retrospective study analysed 323 consecutive patients with GBS who underwent rigid choledochoscopic gallbladder-preserving cholecystolithotomy to determine the detection rate, clinical features, and potential risk factors of gallbladder intramural stones (IS). IS were found in 24.1% (78/323) of patients, characterised by distinct cholangioscopic findings, including stone shadows, yellow floating bands, or a combination of both within the gallbladder wall. Compared to patients without IS, those with IS had a higher prevalence of *Clonorchis sinensis* (*C. sinensis*) eggs (60.3% vs. 40.8%, $P < 0.05$) and elevated serum cholesterol, LDL cholesterol, and Apo-B levels ($P < 0.05$). However, stone composition and *C. sinensis* egg detection rates did not differ between intraluminal stones and IS within the same patient ($P > 0.05$). Logistic regression analysis revealed that IS were associated with *C. sinensis* infection and elevated Apo-B levels. In conclusion, IS share homology with intraluminal stones in the same patient with GBS and exhibit unique appearances in rigid choledochoscopy. For patients with GBS and IS, elevated serum Apo-B levels and *C. sinensis* infection were independent risk factors.

Keywords Gallbladder stones, Intramural stones, Choledochoscopic gallbladder-preserving cholecystolithotomy, *Clonorchis sinensis*, Apolipoprotein B

Gallbladder stones (GBS) are a common and widespread condition worldwide. In clinical practice, GBS are often defined as stones found in the gallbladder lumen. Abdominal ultrasonography, clinical symptoms, and liver biochemistry are the primary methods used to diagnose GBS^{1–4}. Laparoscopic cholecystectomy (LC) is currently the standard surgical procedure for treating GBS^{5–9}. In recent years, a surgical procedure for GBS treatment known as “endoscopic gallbladder-preserving cholecystolithotomy (EGPCL)” has emerged in China^{10–15}. The purpose of EGPCL is to maximise the preservation of a functional gallbladder while removing stones and polyps. Therefore, a thorough diagnostic examination of the gallbladder lumen and wall is necessary during the procedure. In exceptional cases, such as the intraoperative detection of potentially malignant lesions in the gallbladder wall tissue, gallbladder preservation must be abandoned in favour of cholecystectomy.

During rigid choledochoscopic gallbladder-preserving cholecystolithotomy (RCGPCL, a type of EGPCL) for patients with GBS, stones were found in the gallbladder wall (including the mucosal and muscular layers) of some patients. These stones have been referred to as intramural stones (IS), which are considered to be a specific type of GBS in some reports^{16–18}; however, their aetiology and pathogenesis are unknown, and there have been limited clinical investigations to date. In view of this, we retrospectively analysed the clinical data of 323 consecutive patients with GBS who underwent RCGPCL. Our study examines the incidence, clinical characteristics, and risk factors for IS in patients with GBS.

¹Clinical Laboratory, Guangzhou Nansha People’s Hospital, No.7 Xingye Road, Dagang Town, Nansha District, Guangzhou, Guangdong, China. ²Department of Pathology, Guangzhou Nansha People’s Hospital, No. 7 Xingye Road, Dagang Town, Nansha District, Guangzhou, Guangdong, China. ³General Surgery, Guangzhou Nansha People’s Hospital, No. 7 Xingye Road, Dagang Town, Nansha District, Guangzhou, Guangdong, China. ⁴Dongguan Nancheng Hospital, No. 55, Nancheng Avenue, Guantai Road, Dongguan, Guangdong, China. ⁵The Second People’s Hospital of Guangzhou Panyu District, No.88 Guangdong Road, Dashi Street, Panyu District, Guangzhou, Guangdong, China. ✉email: luoxb1976@163.com; Wsgwkys@163.com; fqj1958@163.com

Methods

Ethics statement

Written informed consent was obtained from all participants, including guardians of minors/children involved in the study. This study was approved by the Medical Ethics Committee of the Sixth People's Hospital of Nansha, Guangzhou. All methods were performed in accordance with the relevant guidelines and regulations of the Guangdong Clinical Laboratory Center.

Participants

Altogether, 323 patients underwent RCGPCL implantation between January and December 2011 in the Department of General Surgery at our hospital. There were 171 males and 142 females, with ages ranging from 10 to 80 years and a median age of 45 years, as shown in Table 1. The inclusion criteria were symptomatic GBS or GBS combined with gallbladder polyps.

The exclusion criteria were as follows: (1) patients with simple gallbladder polyps; (2) patients with malignant gallbladder tumours; (3) patients in the acute inflammatory phase of gallbladder disease; and (4) patients with combined obstructive jaundice.

Diagnosis of gallbladder IS

The gallbladder wall was examined intraoperatively using a CHiAO rigid three-channel cholecystoscope (Chinese Patent No. ZL200810026985.X). Stones found within the gallbladder wall (including the mucosal, submucosal, and muscular layers) served as the basis for IS diagnosis.

The specific surgical procedure was as follows: the patient was positioned supine with the head up at 10°–15° and the body tilted 15° to the left. General anaesthesia was administered via tracheal intubation or venipuncture using a laryngeal mask. A 0.6-cm incision was made below the umbilical edge, and a 5.5-mm trocar was inserted to establish pneumoperitoneum at a pressure of 10 mmHg. A laparoscope (Φ , 3–5 mm) was then inserted to explore the abdominal cavity; determine the position, morphology, and size of the gallbladder; and determine any adhesions to other organs. A 1.5- to 2-cm incision was subsequently made under the costal margin nearest to the bottom of the gallbladder. The bottom portion of the gallbladder with few blood vessels was grasped and stabilised under laparoscopic guidance. The laparoscope and trocar were then removed. Next, a 0.8-cm incision was made in the gallbladder with an electric knife, and bile was drawn into the syringe connected to the ventricular drainage tube.

The edge of the incision was clipped using three mosquito forceps in an equilateral triangle, a single-channel or three-channel cholecystoscope was inserted, and 0.9% NaCl was injected to fill the gallbladder and identify the gallbladder cavity. Large stones ($\Phi \geq 0.5$ cm) were removed using a stone extraction basket; small stones ($\Phi < 0.5$ cm), bile sludge, and sand-like stones were extracted with a sludge-like stone-absorbing box. Large stones that could not be caught by the stone extraction basket were fragmented using air-pressure ballistic lithotripsy and then removed by the stone extraction basket or sludge-like stone-absorbing box. After removing all stones from the gallbladder cavity, a sludge-like stone-absorbing box was placed on top of the cholecystoscope. The box clears bile sludge or tiny stones adhered to the gallbladder mucosa and IS using the special techniques of pushing, squeezing, and pressing.

Subsequently, the gallbladder cavity was explored repeatedly using a cholecystoscope to ensure there were no residual stones. Finally, the bottom incision of the gallbladder was closed with double interlocking sutures (3–0 absorbable catgut). The suture was ensured to be tight, and the abdominal wall was sutured layer by layer.

Based on these diagnostic results, patients were categorised into a GBS group or GBS combined with IS (GBS + IS) group for subsequent comparative analysis.

Specimen collection

A 3–5 mL fasting venous blood sample was drawn 48 h before surgery and sent for testing. Gallbladder bile and stones (including IS) were obtained aseptically during surgery. Bile specimens were placed in sterile tubes containing 1% heparin and sent for testing or temporarily stored at 4 °C for no more than 6 h if immediate testing was not possible. Stone specimens were placed in sterile, dry containers for testing. The blood was tested within 6 h after delivery, bile was tested within 24 h, and the remaining specimen was stored in the refrigerator at -80 °C; stones were tested within 72 h, and excess stones were placed in clean and dry glass containers, and stored in ventilated conditions for a long time.

Age (Years)	Solitary stone		Multiple stones		Total
	Male	Female	Male	Female	
~29	4	7	8	16	35
30–39	23	16	23	16	78
40–49	26	17	29	17	89
50–59	18	11	19	19	67
60~	9	18	12	15	54
Total	80	69	91	83	323

Table 1. Distribution of age, sex, and stone type in all patients ($n = 323$).

Specimen testing and methods

Microscopic examination of bile for Clonorchis sinensis (C. sinensis) eggs

We obtained 3 mL of bile, centrifuged at 5000 r/min for 10 min, discarded the upper layer, retained 300 μ L of precipitate, and smeared onto 2–3 slides for microscopic examination.

Microscopic examination of stones for C. sinensis eggs

GBS (including IS) were rinsed twice with distilled water and dried in an oven at 60 °C for 12 h. The stones were cut with a scalpel, and 10 mg (or the whole stone if < 10 mg) was put into a mortar, ground evenly, and mixed with 300 μ L of saline. The suspension was filtered through 260-mesh nylon gauze, and 2–3 slices of smears were taken for microscopic examination. An OLYMPUS BX51 optical microscope and its accompanying microscope camera system (TWIN-DP25, Japan) were used.

C. sinensis eggs in bile and/or stones were observed microscopically to diagnose *C. sinensis* infection in patients.

Stone component analysis

A 2 mg sample of each stone layer was weighed if the layered structures were distinct. For amorphous stones, 2 mg samples were weighed directly. Samples were mixed with potassium bromide (KBr) at 1:150 ratio, ground thoroughly, and pressed into discs. The main components were analysed using a Bruker (TENSOR27, Germany) FTIR spectrometer in the frequency range of 400–4000 cm^{-1} at 4 cm^{-1} resolution.

Scanning electron microscopy (SEM) of stones

A portion of the dried stone samples or several grains of IS were obtained, fixed on the carrier stage with conductive adhesive, sprayed with gold, and examined using a scanning electron microscope (LIS10, ZEISS, Germany).

Assays for blood samples

Serum glucose, triglycerides, total cholesterol, low-density lipoprotein (LDL) cholesterol, and apolipoprotein B (Apo-B) levels were determined using commercially available kits (Beijing Zhongsheng Biotechnology Company, China) via the following methods: glucose (glucokinase-colourimetric assay), triglycerides (phosphoglycerol oxidase-colourimetric assay), total cholesterol (cholesterol oxidase [COD-PAP] assay), LDL cholesterol (direct-assay method), and Apo-B (immunoturbidimetric assay). A TBA-120FR automated biochemistry analyser (Toshiba, Japan) was used.

Statistical analysis and inclusion of possible risk factors for developing IS in patients with GBS

The statistical software (SPSS 17.0) was used to analyse the data. If the quantitative index data of the two samples were normally distributed, an independent sample t-test was used to determine whether there was any difference in the means, and nonparametric tests were used if the data distribution was skewed. Moreover, the chi-squared (χ^2) test was used for comparison of the rate or composition ratio, and the risk factors (odds ratio) were analysed using binary logistic regression.

Results

Intraoperative findings and management of IS in the gallbladder wall

Intraoperative identification of IS

The intraoperative detection of IS during cholecystoscopy depends on three characteristics of the gallbladder wall. First, 'stone shadow': the gallbladder mucosa is locally bulging with isolated or clustered stones embedded within or under the mucosa (referred to as a 'nest'). This characteristic was observed in 466 nests, accounting for 74.3% of cases. Second, 'yellow floating band': a clear yellow flocculent band floating on the mucosa, difficult to remove and becomes more obvious when squeezed. When the mucosa is incised using a lithotripter, IS are found. This feature was present in 98 nests (15.7%). Third, 'stone shadow' combined with 'yellow floating band': 'stone shadow' and 'yellow floating band' appearing simultaneously within the mucosa of the gallbladder wall. This combination was identified in 63 nests, accounting for 10% of cases (Fig. 1A).

Surgical removal of IS

IS identified using the above means can be discharged into the gallbladder cavity by combining cholecystoscopy and a special IS suction box with pushing, squeezing, pressing, tearing, propping, punching, and suctioning, after which the IS can be extracted using negative-pressure suction box technology (Fig. 1B). Among the 323 patients with GBS included in this study, 78 had combined IS with a detection rate of 24.1%. In addition, 627 IS nests were removed during surgery, with a minimum of one nest and a maximum of 56 nests, averaging 7.9 nests. Most extracted IS were irregular, gravelly, and black or brown, typically measuring less than 1 mm in diameter, though a few exceeded 3 mm (Fig. 1C).

The different locations of IS in the gallbladder of the 78 patients were as follows: 1.3% (1/78), 3.8% (3/78), and 76.9% (60/78) were found in the neck, bottom, and body of the gallbladder, respectively; 6.4% was found in both the body and bottom (5/78); 10.3% was found in both the body and neck (8/78); and 1.3% was simultaneously found in the bottom, body, and neck (1/78), as shown in Fig. 1D. Overall, the gallbladder body (body alone and two or more locations, including the body; Fig. 4) accounted for 94.5% (74/78) of IS cases.

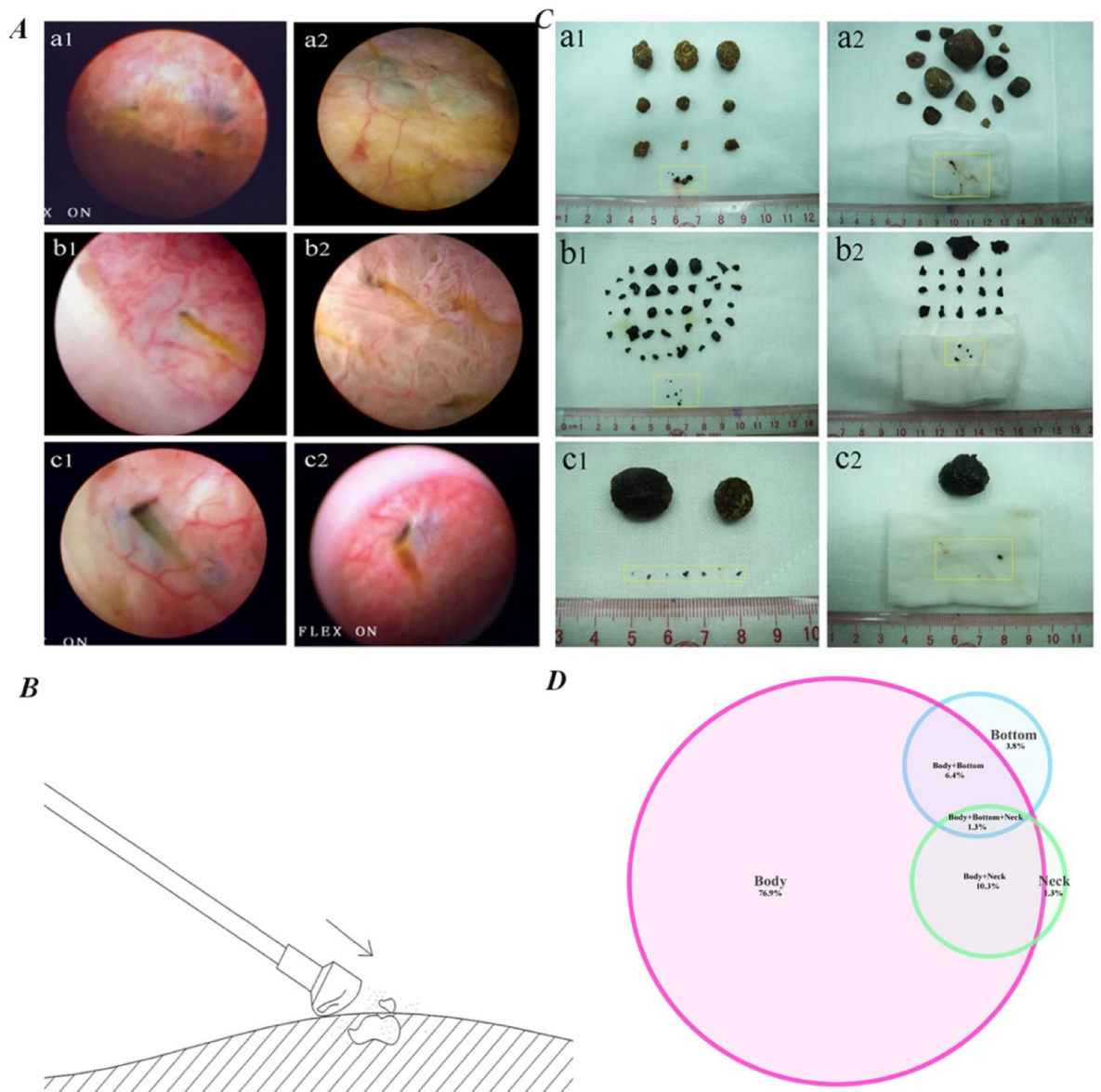


Fig. 1. Observation, diagnosis, and removal of gallbladder intramural stones (IS) using rigid choledochoscopy. **(A)** Three endoscopic features of IS: a1, a2: black or blue-black stone shadows; b1, b2: yellow floating band sign; c1, c2: stone shadows with a yellow floating band sign. **(B)** Schematic diagram of the choledochoscope used in conjunction with a specialised lithotripsy box for IS removal via pushing, squeezing, and compression techniques. **(C)** Gallbladder stones removed intraoperatively, including intraluminal stones and IS (highlighted in light yellow boxes), corresponding to stone shadows (a1, a2), yellow floating band sign (b1, b2), and stone shadows with a yellow floating band sign (c1, c2). **(D)** Distribution of IS at different locations within the gallbladder wall.

Comparison of the IS and gallbladder intraluminal stone composition from the same patient

As shown in Fig. 1C, most IS were tiny, brittle black particles with a black cross-section (pigment stones); nevertheless, some were brown or yellowish particles (cholesterol stones) or both (mixed stones). The appearance of intraluminal stones varied depending on composition: pigment stones were black or brown with a rough, granular surface, brittle texture, and smaller diameter; cholesterol stones were yellowish or light brown, polyhedral or spherical, with a rough or smooth surface and a larger diameter; mixed stones displayed various colours, shapes and textures depending on calcium content.

The composition of IS and intraluminal stones in these 78 patients was analysed (the infrared spectra of the different stone compositions are shown in Fig. 2A). Results showed that the composition ratios of cholesterol, pigment, and mixed cholesterol-pigment stones among IS were 10.2%, 71.7%, and 18.1%, respectively, and the stone compositions of matching intraluminal stones were 11.8%, 69.3%, and 18.9%, respectively. The compliance rate of the stone composition types of IS and intraluminal stones was 94.8%, and that of *C. sinensis* egg detection

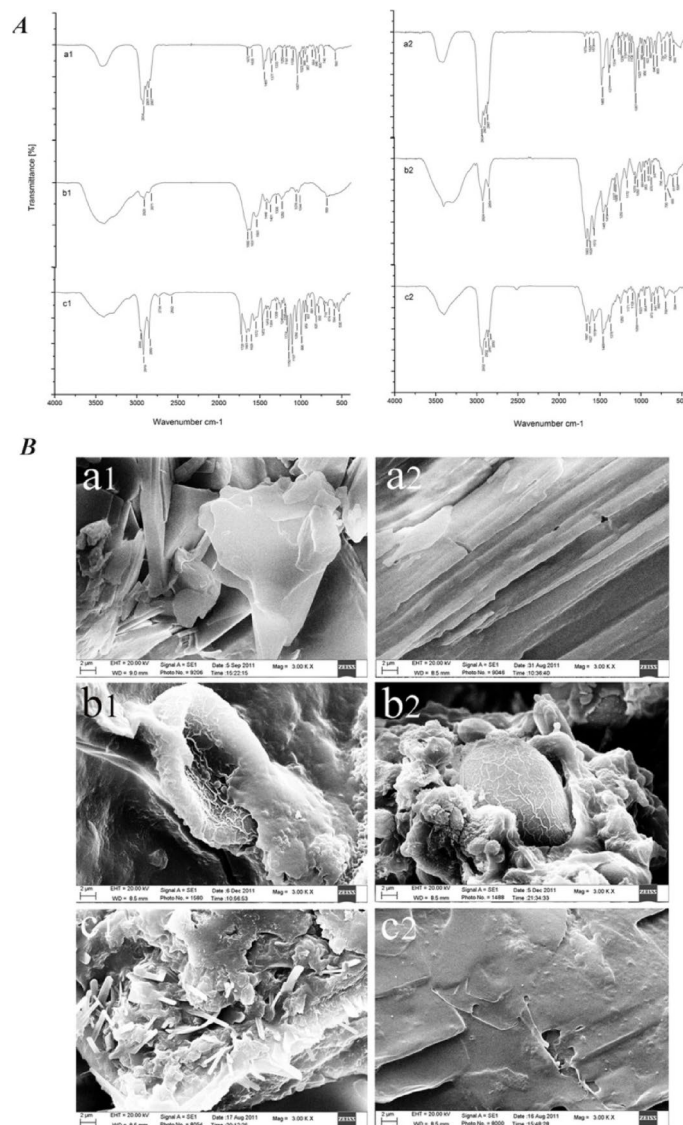


Fig. 2. Fourier transform infrared spectroscopy (FTIR) analysis and scanning electron microscopy (SEM) observation of IS (a1, b1, c1) and gallbladder intraluminal stones (a2, b2, c2) from the same patient. **(A)** The infrared (IR) spectrum of stones with different compositions. a1, a2: IR spectrum of cholesterol stones. b1, b2: IR spectrum of pigment stones. c1, c2: IR spectrum of cholesterol-pigment mixed stones. **(B)** Microstructures of stones under SEM. Stones (a1, a2) are cholesterol stones exhibiting plate-like cholesterol crystals; b1, b2 are pigment stones, with irregular particles encasing the *Clonorchis sinensis* (*C. sinensis*) egg in the intraluminal stone (b2) and mucus-like material encasing the egg in IS (b1). c1, c2 are mixed stones, with c1 being an IS showing striated cholesterol crystals encapsulated by irregular bilirubin particles and c2 being an intraluminal stone with slate-like cholesterol crystals with some irregular bilirubin particles adhering to the surface.

was 98.7%, as shown in Table 2. Similarly, Fig. 2B illustrates that the microstructures of intraluminal stones and IS from the same patient were nearly identical under SEM.

Association between *C. sinensis* egg detection and gallbladder IS

Among the 323 patients with GBS, *C. sinensis* eggs were detected in the bile and/or stones of 147 patients, with a detection rate of 45.5%. Of the 147 patients, 47 (32.0%) had IS. In contrast, only 31 (17.6%) of the 176 patients in whom no *C. sinensis* eggs were detected had IS (Fig. 3B). Furthermore, *C. sinensis* eggs were found in 60.3% (47/78) of patients with IS, which was higher than the 40.5% (100/245) observed in patients without IS ($P < 0.05$, Fig. 3C).

Under SEM, *C. sinensis* eggs in IS were mostly encapsulated by a mucus-like material, with the contents not clearly visible. Bilirubin particles and/or calcium carbonate crystals were adsorbed on the surface and periphery of the eggs. Some eggs were deformed, depressed, or had lost their caps (Fig. 3A).

Stone type	Cholesterol stone		Pigment stone		Mixed stone		Total
	Pos.	Neg.	Pos.	Neg.	Pos.	Neg.	
Intramural stones	1	7	41	15	5	9	78
Intraluminal stones	1	8	42	12	5	10	78
Total	2	15	83	27	10	19	156

Table 2. Intramural and intraluminal stones from the same patients were compared in terms of stone type composition and the presence of *C. sinensis* eggs (n). Pos. and Neg. indicated positive or negative results for *C. sinensis* eggs.

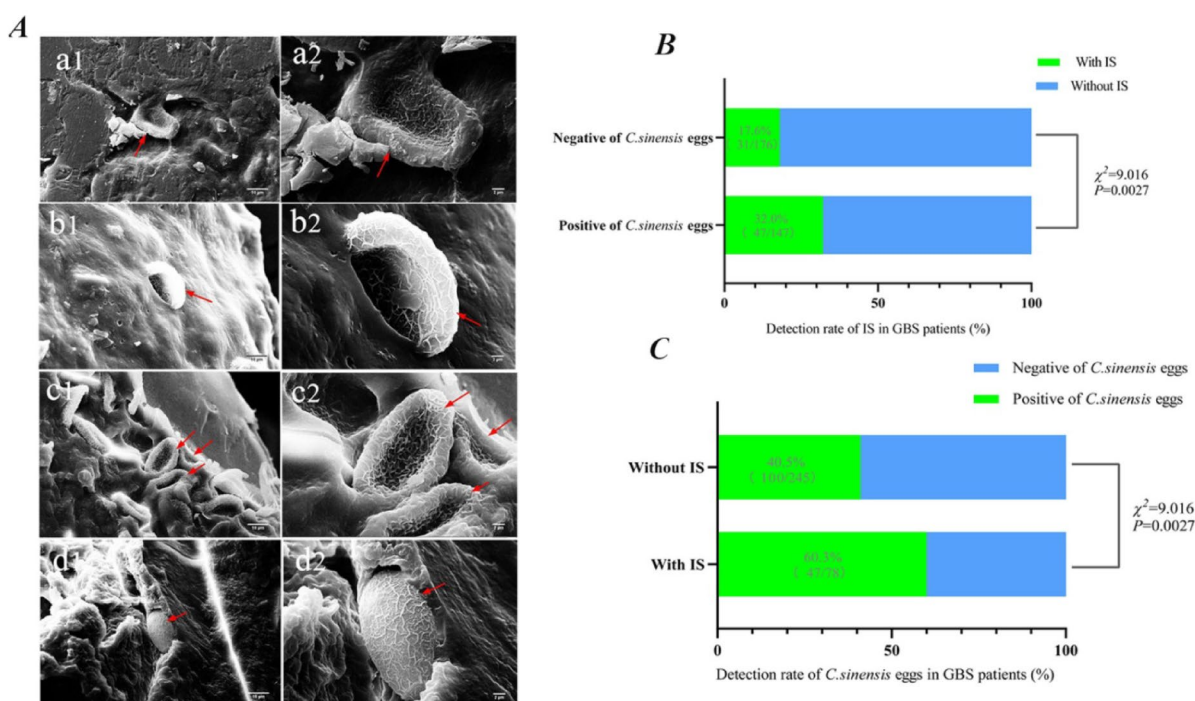


Fig. 3. Morphology of *C. sinensis* eggs in intramural stones (IS) was examined using SEM, as well as the connection between the eggs' presence and IS formation. (A) *C. sinensis* eggs' morphology seen by SEM in IS (indicated by red arrows): eggs aggregated or embedded in the stone looked deformed and were encased in a mucus-like material. The pictures a2, b2, c2, and d2 are magnified images corresponding to a1, b1, c1, and d1. (B) Comparison of IS incidence between patients with and without detectable *C. sinensis* eggs. (C) Comparison of *C. sinensis* egg detection rates in patients with and without concurrent IS.

Changes in blood glucose and lipids in patients with IS

Blood glucose, triglycerides, total cholesterol, LDL cholesterol, and Apo-B levels were analysed and compared among patients with GBS ($n=226$) and patients with GBS and IS (GBS+IS) ($n=77$) after excluding patients who had not undergone testing. Figure 4A illustrates that total cholesterol, LDL cholesterol, and Apo-B levels were higher in patients with GBS+IS ($P<0.01$). However, blood glucose and triglyceride levels did not differ significantly between the two groups ($P>0.05$).

Evaluating the risk factors for patients with GBS and IS

C. sinensis infection, elevated serum total cholesterol, LDL cholesterol, and Apo-B levels were all included in a binary logistic regression analysis along with age, sex, hepatitis B virus infection, stone type (single or multiple), medical history, and intraluminal stone size to determine whether they were risk factors for the development of IS in patients with GBS. By analysis, IS occurrence in patients with GBS was not associated with age, sex, total cholesterol, LDL cholesterol concentration, hepatitis B virus infection, stone type, medical history, or the stone size. However, *C. sinensis* infection (OR = 2.118, 95% CI = 1.241–3.614, $P=0.006$) and Apo-B levels (OR = 2.271, 95% CI = 1.234–4.180, $P=0.008$) were independent risk factors for IS occurrence in patients with GBS patients, as detailed in Fig. 4B.

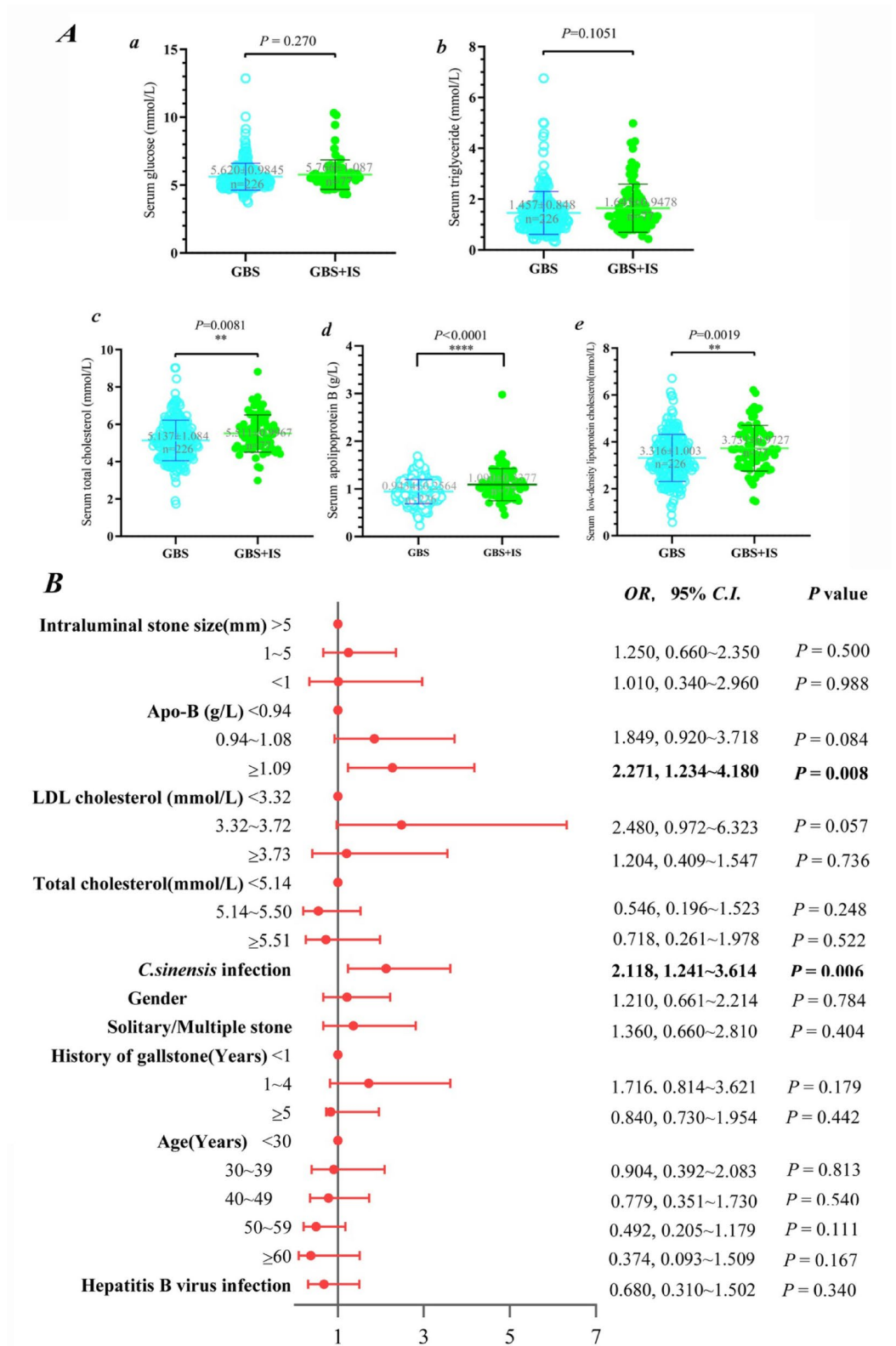


Fig. 4. (A) Serum glucose (a), triglyceride (b), total cholesterol (c), apolipoprotein B (d), and LDL cholesterol (e) concentrations were compared between patients with gallbladder stones (GBS group) and patients with both gallbladder stones and IS (GBS + IS group). ** $P < 0.01$, **** $P < 0.0001$. (B) Association of different factors with IS occurrence in patients with gallbladder stones. OR: odds ratio. CI: confidence interval.

Comparison of three-year postoperative recurrence rates in patients with GBS with and without IS

Owing to incomplete follow-up data, we reviewed the relatively complete follow-up data of 325 patients with GBS who underwent RCGPCL between January and December 2012. The occurrence of IS intraoperatively and its relationship with postoperative stone recurrence were analysed. After survival analysis and Kaplan–Meier test, there was no difference in three-year recurrence rates (36 months) after surgery in 117 patients with GBS and IS (16.1% vs. 20.9%, $\chi^2=0.584$, $P=0.445$) compared with the 208 patients with GBS, as detailed in Fig. 5.

Discussion

IS, also known as submucosal stones, are a distinct type of gallbladder stone found within the mucosal, muscular, and plasma layers of the gallbladder^{19–22}. However, because IS are usually embedded in the gallbladder wall, surface ultrasonography cannot detect them, and postoperative pathologic examination or endoscopic surgery is frequently used to make the diagnosis^{16–18}.

The presence of IS in the gallbladder wall, and its three distinctive choledochoscopic features—stone shadow, yellow fluttering band, and a combination of both—were observed using choledochoscopy. The stones were then extracted from the gallbladder wall at appropriate locations (Fig. 1). As shown in Table 2, IS presenting with a “black or blue-black stone shadow” were all black pigment stones (formed by the oxidation of bilirubin and metal ions such as calcium and iron) accumulated in clusters within the mucous membrane layer or submucosa and formed what we termed a “nest”. In addition, those IS presenting as a “yellow floating band” were mostly brown or tan pigmented stones or yellowish cholesterol-pigment mixed stones, which appear as striated aggregates in the mucosal or submucosa layers.

Moreover, we found that IS predominantly occur in the gallbladder body and rarely in the neck alone, which may be related to the anatomical and physiological functions of the gallbladder, such as the greater size of the body, its inherent elasticity, as well as the associated secretion and storage of mucus, concentration, and emptying of bile^{23–26}. A high degree of concordance was observed when the composition and microstructure of intraluminal stones and IS were obtained from the same patient (Table 2; Fig. 2), indicating that the conditions or causes of their development were essentially the same. In other words, there is an extent of homology between intraluminal stones and IS from the same patient. Further research is necessary to determine why IS with various pigment and chemical compositions exhibit distinct aggregation patterns within the gallbladder wall.

The pathogenesis and mechanisms of IS remain unknown, and the relationship between *C. sinensis* infection and IS has not yet been reported. Our findings indicated that *C. sinensis* infection is an independent risk factor for patients with GBS and IS (OR=2.118, 95% CI=1.241–3.614, $P=0.006$). *C. sinensis* is a zoonotic disease contracted by consuming raw or semi-raw freshwater fish and shrimp containing live metacercariae. It primarily causes hepatobiliary lesions in the liver and bile ducts of humans and is endemic to Asia, including China, Japan, the Korean Peninsula, Vietnam, and other Southeast Asian countries^{27–29}. Previous studies have reported a strong association between GBS and *C. sinensis* infection^{30–32}. In this study, we consistently detected *C. sinensis* eggs in both intraluminal stones and IS in the same patient, with a 98.7% compliance rate (Table 2). This implies that the function of *C. sinensis* eggs in the development of IS is similar to that of intraluminal stone formation. Infection with *C. sinensis* leads to the accumulation of mucous materials, causing the gallbladder bile to become viscous and difficult to empty. This excessive mucus production could be related to the inflammatory response of the gallbladder wall triggered by metabolites and mechanical stimulation from adult worms and eggs^{33–35}. Furthermore, because of their tiny size and uneven surface mesh, *C. sinensis* eggs are deposited by gravity and bile eddy currents, allowing them to remain in the mucus-covered folds of the gallbladder mucosa for an extended period. Under certain conditions, these eggs deform, die, and calcify, penetrating the mucosa and even muscular layers of the gallbladder to form IS (Figs. 2B and 3A). This observation was further supported by the detection of *C. sinensis* eggs in several gallbladder wall specimens sent for pathological analysis (Fig. 6A).

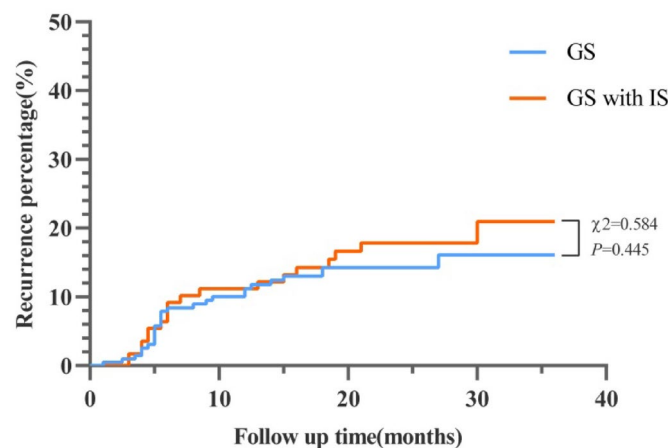


Fig. 5. Comparison of three-year postoperative recurrence rate between patients with gallstone and those with IS and gallstone. GS: patients with gallstone; GS with IS: patients with gallstone and intramural stones.

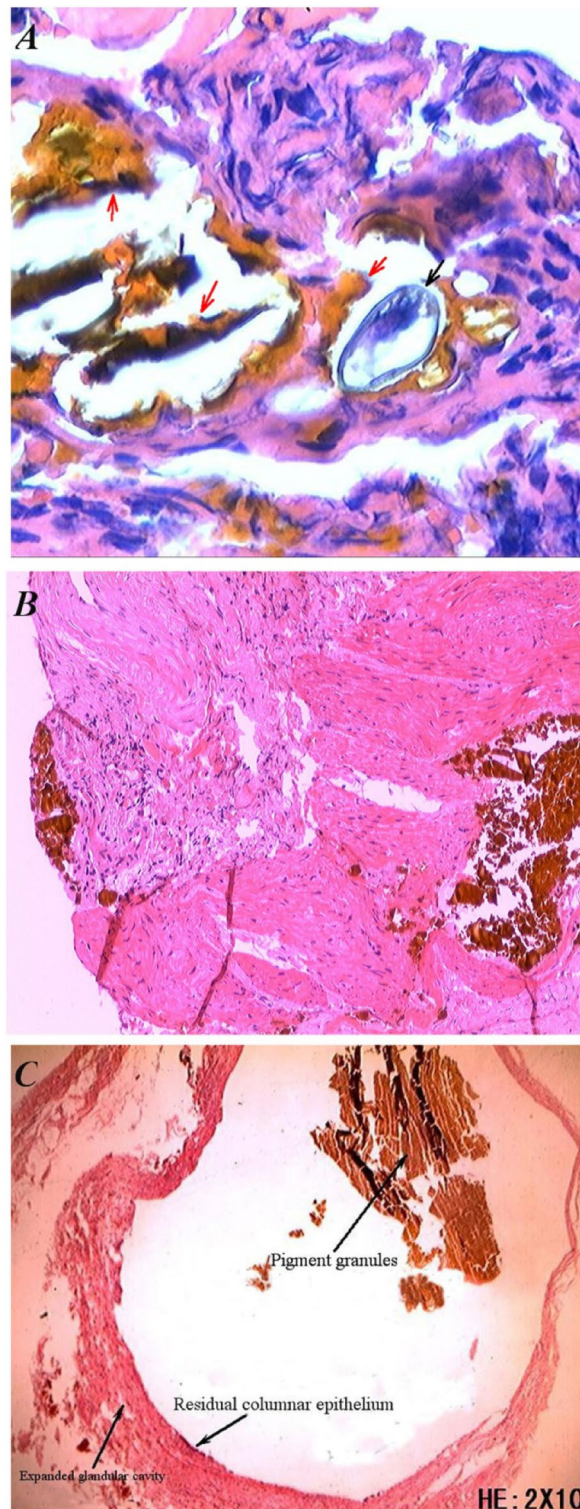


Fig. 6. *C. sinensis* eggs and IS observed by pathological examination of the gallbladder wall tissue (hematoxylin-eosin staining). (A) *C. sinensis* eggs (black arrows) and pigment granules (red arrows) within the gallbladder wall at 400× magnification; (B) Pigment granules localised in the mucosal or submucosal layers of the gallbladder wall at 20× magnification; (C) Dilated Rokitansky-Aschoff sinus observed within the gallbladder wall encasing pigment granules and forming a diverticulum, magnification 20×.

In addition, some clinical studies have reported that patients with xanthogranulomatous cholecystitis often have pigment material or small stones in the gallbladder wall^{36–39}. The long-term activation of inflammation that damages the mucosal basal layer and allows bile to permeate into the muscularis propria in the gallbladder lumen may be the cause of the formation of tiny pigment stones in the gallbladder wall^{36–39} (Fig. 6B). However, we were unable to determine whether the pathogenic mechanisms causing xanthogranulomatous cholecystitis and the appearance of IS induced by *C. sinensis* infection were the same.

The probability and risk factors for IS in patients with GBS from non-endemic regions may differ because of the widespread geographic distribution of *C. sinensis* infection. In addition to *C. sinensis* infection, elevated serum Apo-B (≥ 1.09 g/L) has also been identified as an independent risk factor for IS formation (Fig. 4B). GBS is associated with elevated serum Apo-B^{40–42}. Apo-B is primarily synthesised by the liver and is the main apolipoprotein for transporting VLDL and LDL^{43–45}. Its elevation impacts hepatic bile acid synthesis and secretion⁴⁶ and can be directly excreted into bile, disrupting cholesterol transport vesicle stability and promoting cholesterol crystal formation^{47,48}. This process ultimately leads to cholesterol stone formation. Excess serum Apo-B concentration has also been associated with the production and deposition of cholesterol crystals in localised tissues, such as the joint cavities of patients with rheumatoid arthritis^{49,50} and the vessel walls of patients with atherosclerosis^{51–53}. Because Apo-B is present in bile and the gallbladder wall^{47,48,54}, its elevation under certain conditions, such as during chronic inflammation and increased glycoprotein or mucus secretion, may cause local cholesterol transport impairment as well as cholesterol crystal production and deposition. However, owing to the limitations of this study, these postulated pathological mechanisms remain to be confirmed.

Multiple studies have shown that patients with gallbladder adenomyosis develop a distinctive diverticulum-like structure called the Rokitansky-Aschoff sinus (R-A sinus), which frequently contains deposits of pigment granules and cholesterol crystals^{19,55–57}. The prevailing consensus is that the R-A sinus is a consequence of chronic cholecystitis, which is characterised by increased mucus production and epithelial hyperplasia^{58–60}. Elevated cholestasis pressure in the gallbladder lumen allows bile to enter the RA sinus, where it expands into a cyst or diverticulum that may penetrate deep into the muscularis propria. Consequently, crystals or pigmented particulate matter are deposited in the enlarged sinus along with mucous material that surrounds the adhesion, forming microstones^{61,62}. Similarly, pigment granules were observed in several gallbladder walls within the glandular lumen of sunken gallbladder mucosa and within the dilated R-A sinus (Fig. 6C). However, more clinical research is required to determine the relationship between gallbladder adenomyosis and IS, as well as to clarify whether the small stones identified in the R-A sinus are IS discovered post-surgery.

Additionally, it is important to follow up and evaluate the impact of IS on stone recurrence in patients with gallbladder stones undergoing RCGPCL. The results indicated that three years post-surgery, patients with GBS and IS exhibited stone recurrence rates similar to those with simple gallstones (Fig. 5); all IS and intraluminal stones from the patients in this study were surgically removed. Furthermore, a sizable proportion of patients were lost to follow-up after three years, which is a limitation of this study that may result in differences in long-term follow-up outcomes.

This study concludes that there is homology between gallbladder IS and intraluminal stones within the same patient, that choledochoscopy-observed characteristics of gallbladder IS are distinctive, and that elevated serum Apo-B and *C. sinensis* infection are independent risk factors for patients with GBS combined with IS. Clinical surgeons should consider the presence of IS, *C. sinensis* infection (only in endemic areas), and changes in serum lipid metabolism when performing gallbladder stone surgeries. This will facilitate prompt detection intervention, thereby preventing the development of complications beyond gallstones.

Data availability

All data generated or analyzed during this study are included in this published article.

Received: 5 October 2024; Accepted: 30 April 2025

Published online: 08 May 2025

References

- Lammert, F. et al. Gallstones. *Nat. Rev. Dis. Primers.* **2**, 16024 (2016).
- Lee, J. Y., Keane, M. G. & Pereira, S. Diagnosis and treatment of gallstone disease. *Practitioner* **259**, 15–19 (2015).
- Cremer, A. & Arvanitakis, M. Diagnosis and management of bile stone disease and its complications. *Minerva Gastroenterol. Dietol.* **62**, 103–129 (2016).
- Gutt, C., Schäfer, S. & Lammert, F. The treatment of gallstone disease. *Dtsch. Arztebl Int.* **117**, 148–158 (2020).
- Hoozemans, J. B., Groen, A. K. & de Brauw L. M. Laparoscopische cholecystolithotomie [laparoscopic cholecystolithotomy]. *Ned. Tijdschr. Geneesk.* **21**, D6658 (2022).
- Ripetti, V., Luffarelli, P., Santoni, S. & Greco, S. Laparoscopic cholecystectomy: do risk factors for a prolonged length of stay exist? *Update Surg.* **71**, 471–476 (2019).
- Omar, M. A., Redwan, A. A. & Mahmoud, A. G. Single-incision versus 3-port laparoscopic cholecystectomy in symptomatic gallstones: A prospective randomised study. *Surgery* **162**, 96–103 (2017).
- Boerma, D. & P Schwartz, M. Gallstone disease. Management of common bile-duct stones and associated gallbladder stones: surgical aspects. *Best Pract. Res. Clin. Gastroenterol.* **20**, 1103–1116 (2006).
- Malik, F. S. et al. Laparoscopic cholecystectomy in situs inversus totalis. *J. Coll. Physicians Surg. Pak.* **29**, 1000–1002 (2019).
- Tan, Y. Y. et al. A new strategy of minimally invasive surgery for cholecystolithiasis: calculi removal and gallbladder preservation. *Dig. Surg.* **30**, 466–471 (2013).
- Liu, J. et al. A new operation for gallstones: choledochoscopic gallbladder-preserving cholecystolithotomy, a retrospective study of 3,511 cases. *Surgery* **172**, 1302–1308 (2022).
- Qu, Q. et al. Role of gallbladder-preserving surgery in the treatment of gallstone diseases in young and middle-aged patients in China: results of a 10-year prospective study. *Surgery* **167**, 283–289 (2020).
- Ullah, S. et al. Are laparoscopic cholecystectomy and natural orifice transluminal endoscopic surgery gallbladder preserving cholecystolithotomy truly comparable? A propensity matched study. *World J. Gastrointest. Surg.* **14**, 470–481 (2022).

14. Shang, L. et al. Update on the natural orifice transluminal endoscopic surgery for gallbladder preserving gallstones therapy: a review. *Med. (Baltim)*. **101**, e31810 (2022).
15. He, X. J. et al. Gallbladder-preserving polypectomy for gallbladder polyp by embryonic-natural orifice transumbilical endoscopic surgery with a gastric endoscopy. *BMC Gastroenterol.* **22**, 216 (2022).
16. Kawanishi, K. & Nishimura, F. Intramural pure pigment gallstones. A case report. *Acta Med. Okayama*. **17**, 203–207 (1963).
17. Mizuno, T. et al. Intramural giant Gallstone: report of a rare case. *Am. J. Gastroenterol.* **82**, 454–456 (1987).
18. Iwamura, K. & Ueno, F. Laparoscopic finding of the gallbladder in a case of intramural gallstones. *Gastroenterol. Jpn.* **13**, 442–446 (1978).
19. Graif, M., Horovitz, A., Itzhak, Y. & Strauss, S. Hyperechoic foci in the gallbladder wall as a sign of microabscess formation or diverticula. *Radiology* **152**, 781–784 (1984).
20. Yosepovich, A., Nass, D., Zagatsky, M. & Koplovic, J. Chronic cholecystitis with bone metaplasia. A case report. *Pathol. Res. Pract.* **198**, 765–766 (2002).
21. Muto, Y., Uchimura, M., Waki, S., Sameshima, Y. & Ishigaki, J. Relationship between bilocular (Hourglass) gallbladder to intramural stones of the gallbladder. *Rinsho Hoshasen*. **20**, 663–672 (1975). Japanese.
22. Apostolidis, S., Zatagias, A. & Zevgaridis, A. Intramural gallstones mimicking typical lithiasic cholecystitis. *South. Med. J.* **104**, 59–60 (2011).
23. Jackowiak, H. & Lametschwandner, A. Angioarchitecture of the rabbit extrahepatic bile ducts and gallbladder. *Anat. Rec Discov Mol. Cell. Evol. Biol.* **286**, 974–981 (2005).
24. Bird, N. C., Wegstapel, H., Chess-Williams, R. & Johnson, A. G. In vitro contractility of stimulated and non-stimulated human gallbladder muscle. *Neurogastroenterol Motil.* **8**, 63–68 (1996).
25. Fuchs, W. S. et al. Effect of gallbladder contraction induced chologogia on the Pharmacokinetic profile of a sustained-release Theophylline formulation. *Arzneim Forsch.* **46**, 1120–1126 (1996).
26. Housset, C., Chrétien, Y., Debray, D. & Chignard, N. Functions of the gallbladder. *Compr. Physiol.* **6**, 1549–1577 (2016).
27. Kim, T. S., Pak, J. H., Kim, J. B. & Bahk, Y. Y. Clonorchis sinensis, an Oriental liver fluke, as a human biological agent of cholangiocarcinoma: a brief review. *BMB Rep.* **49**, 590–597 (2016).
28. Zheng, S. et al. Liver fluke infection and cholangiocarcinoma: a review. *Parasitol. Res.* **116**, 11–19 (2017).
29. Conlan, J. V., Sripa, B., Attwood, S. & Newton, P. N. A review of parasitic zoonoses in a changing Southeast Asia. *Vet. Parasitol.* **182**, 22–40 (2011).
30. Choi, D. et al. Gallstones and Clonorchis sinensis infection: a hospital-based case-control study in Korea. *J. Gastroenterol. Hepatol.* **23**, e399–e404 (2008).
31. Qiao, T., Ma, R. H., Luo, X. B., Luo, Z. L. & Zheng, P. M. Cholecystolithiasis is associated with Clonorchis sinensis infection. *PLOS One*. **7**, e42471 (2012).
32. Qian, M. B. et al. Severe hepatobiliary morbidity is associated with Clonorchis sinensis infection: the evidence from a cross-sectional community study. *PLOS Negl. Trop. Dis.* **15**, e0009116 (2021).
33. Sheung-To, C. & Gibson, J. B. The histochemistry of biliary mucins and the changes caused by infestation with Clonorchis sinensis. *J. Pathol.* **101**, 185–197 (1970).
34. Lee, S. H. et al. Secretions of the biliary mucosa in experimental clonorchiasis. *Korean J. Parasitol.* **31**, 13–20 (1993).
35. Choi, B. I., Han, J. K., Hong, S. T. & Lee, K. H. Clonorchiasis and cholangiocarcinoma: etiologic relationship and imaging diagnosis. *Clin. Microbiol. Rev.* **17**, 540–552 (2004). table of contents.
36. Giudicelli, X., Rode, A., Bancel, B., Nguyen, A. T. & Mabrut, J. Y. Xanthogranulomatous cholecystitis: diagnosis and management. *J. Visc. Surg.* **158**, 326–336 (2021).
37. Makimoto, S. et al. Xanthogranulomatous cholecystitis: a review of 31 patients. *Surg. Endosc.* **35**, 3874–3880 (2021).
38. Saritas, A. G. et al. Xanthogranulomatous cholecystitis: a rare gallbladder pathology from a single-center perspective. *Ann. Surg. Treat. Res.* **99**, 230–237 (2020).
39. Rijal, S. et al. Xanthogranulomatous cholecystitis mimicking gallbladder carcinoma: a case report. *Ann. Med. Surg. (Lond)*. **85**, 1116–1118 (2023).
40. Haal, S. et al. Gallstone formation follows a different trajectory in bariatric patients compared to nonbariatric patients. *Metabolites* **11**, 682 (2021).
41. Morán, S. et al. Association between serum concentration of apolipoproteins A-I and B with gallbladder disease. *Arch. Med. Res.* **34**, 194–199 (2003).
42. Wang, J. et al. Serum lipid levels are the risk factors of gallbladder stones: a population-based study in China. *Lipids Health Dis.* **19**, 50 (2020).
43. Packard, C. J. et al. Apolipoprotein B metabolism and the distribution of VLDL and LDL subfractions. *J. Lipid Res.* **41**, 305–318 (2000).
44. Behbodikhah, J. et al. Apolipoprotein B and cardiovascular disease: biomarker and potential therapeutic target. *Metabolites* **11**, 690 (2021).
45. Mehta, A. & Shapiro, M. D. Apolipoproteins in vascular biology and atherosclerotic disease. *Nat. Rev. Cardiol.* **19**, 168–179 (2022).
46. Hillebrant, C. G., Nyberg, B., Einarsson, K. & Eriksson, M. The effect of plasma low density lipoprotein apheresis on the hepatic secretion of biliary lipids in humans. *Gut* **41**, 700–704 (1997).
47. Sewell, R. B., Mao, S. J., Kawamoto, T. & LaRusso, N. F. Apolipoproteins of high, low, and very low density lipoproteins in human bile. *J. Lipid Res.* **24**, 391–401 (1983).
48. Hattori, Y., Tazuma, S., Yamashita, G. & Kajiyama, G. The comparative potency of cholesterol crystallisation-effector proteins in supersaturated model bile systems: association with vesicle transformation. *J. Gastroenterol. Hepatol.* **13**, 1161–1170 (1998).
49. Ananth, L., Prete, P. E. & Kashyap, M. L. Apolipoproteins A-I and B and cholesterol in synovial fluid of patients with rheumatoid arthritis. *Metabolism* **42**, 803–806 (1993).
50. Lazarevic, M. B. et al. Cholesterol crystals in synovial and bursal fluid. *Semin Arthritis Rheum.* **23**, 99–103 (1993).
51. Lorey, M. B., Öörni, K. & Kovanen, P. T. Modified lipoproteins induce arterial wall inflammation during atherogenesis. *Front. Cardiovasc. Med.* **9**, 841545 (2022).
52. Price, L., Sniderman, A., Omerglu, A. & Lachapelle, K. Bioprosthetic valve degeneration due to cholesterol deposition in a patient with normal lipid profile. *Can. J. Cardiol.* **23**, 233–234 (2007).
53. Iwata, T., Murata, M., Hirose, M. & Shimada, K. Cholesterol pericarditis identified by increased cardiothoracic ratio on chest radiography: a case report. *J. Cardiol.* **48**, 221–226 (2006). Japanese.
54. Pattinson, N. R., Upton, P., Ellingsen, P. J. & Chapman, B. A. Apolipoprotein localisation in the human bile duct and gallbladder. *Pathology* **22**, 55–60 (1990).
55. Bonatti, M. et al. Gallbladder adenomyomatosis: imaging findings, tricks and pitfalls. *Insights Imaging.* **8**, 243–253 (2017).
56. Cetta, F., Lombardo, F. & Malet, P. F. Black pigment gallstones with cholesterol gallstones in the same gallbladder. 13 cases in a surgical series of 1226 patients with gallbladder stones. *Dig. Dis. Sci.* **40**, 534–538 (1995).
57. Terada, T. Histopathologic features and frequency of gall bladder lesions in consecutive 540 cholecystectomies. *Int. J. Clin. Exp. Pathol.* **6**, 91–96 (2013).
58. Lee, H. J., Chung, W. S., Kim, J. Y., An, J. H. & Park, S. Chronic inflammation-related radiological findings of gallbladder adenomyomatosis. *Jpn J. Radiol.* **38**, 463–471 (2020).
59. Pham, H. D., Ngo, M. X. & Dang, T. H. Diffuse gallbladder adenomyomatosis in a child. *Cureus* **13**, e15555 (2021).

60. Abraham, S. C. et al. Diffuse lymphoplasmacytic chronic cholecystitis is highly specific for extrahepatic biliary tract disease but does not distinguish between primary and secondary sclerosing cholangiopathy. *Am. J. Surg. Pathol.* **27**, 1313–1320 (2003).
61. Baig, S. J., Biswas, S., Das, S., Basu, K. & Chattopadhyay, G. Histopathological changes in gallbladder mucosa in cholelithiasis: correlation with chemical composition of gallstones. *Trop. Gastroenterol.* **23**, 25–27 (2002).
62. Cariati, A. & Cetta, F. Rokitansky-Aschoff sinuses of the gallbladder are associated with black pigment gallstone formation: a scanning electron microscopy study. *Ultrastruct Pathol.* **27**, 265–270 (2003).

Acknowledgements

Thanks Dr. Feng Yu-yang, Dr. Huang Yi-min, and Dr. Zhou Ping-yi of Guangzhou Nansha People's Hospital, Guangzhou City, China, for providing the samples and clinical data for the study.

Author contributions

Xiaobing Luo, Hongying Cai and Xiaofeng Wang wrote the main manuscript text, and Gang Wang, Ruihong Ma prepared the Figs. 1, 2 and 3 and Sangui Wang, Tie Qiao guided and revised the article. All authors reviewed the manuscript.

Declarations

Competing interests

The authors declare no competing interests.

Additional information

Correspondence and requests for materials should be addressed to X.L., S.W. or T.Q.

Reprints and permissions information is available at www.nature.com/reprints.

Publisher's note Springer Nature remains neutral with regard to jurisdictional claims in published maps and institutional affiliations.

Open Access This article is licensed under a Creative Commons Attribution-NonCommercial-NoDerivatives 4.0 International License, which permits any non-commercial use, sharing, distribution and reproduction in any medium or format, as long as you give appropriate credit to the original author(s) and the source, provide a link to the Creative Commons licence, and indicate if you modified the licensed material. You do not have permission under this licence to share adapted material derived from this article or parts of it. The images or other third party material in this article are included in the article's Creative Commons licence, unless indicated otherwise in a credit line to the material. If material is not included in the article's Creative Commons licence and your intended use is not permitted by statutory regulation or exceeds the permitted use, you will need to obtain permission directly from the copyright holder. To view a copy of this licence, visit <http://creativecommons.org/licenses/by-nc-nd/4.0/>.

© The Author(s) 2025